

G. Arfeuille · L. A. Mysak · L.-B. Tremblay

Simulation of the interannual variability of the wind-driven Arctic sea-ice cover during 1958–1998

Received: 27 January 1999 / Accepted: 8 July 1999

Abstract A thermodynamic-dynamic sea-ice model based on a granular material rheology developed by Tremblay and Mysak is used to study the interannual variability of the Arctic sea-ice cover during the 41-year period 1958–98. Monthly wind stress forcing derived from the National Centers for Environmental Prediction (NCEP) Reanalysis data is used to produce the year-to-year variations in the sea-ice circulation and thickness. We focus on analyzing the variability of the sea-ice volume in the Arctic Basin and the subsequent changes in sea-ice export into the Greenland Sea via Fram Strait. The relative contributions of the Fram Strait sea-ice thickness and velocity anomalies to the sea-ice export anomalies are first investigated, and the former is shown to be particularly important during several large export events. The sea-ice export anomalies for these events are next linked to prior sea-ice volume anomalies in the Arctic Basin. The origin and evolution of the sea-ice volume anomalies are then related to the sea-ice circulation and atmospheric forcing patterns in the Arctic. Large sea-ice export anomalies are generally preceded by large volume anomalies formed along the East Siberian coast due to anomalous winds which occur when the Arctic High is centered closer than usual to this coastal area. When the center of this High relocates over the Beaufort Sea and the Icelandic Low extends far into the

Arctic Basin, the ice volume anomalies are transported to the Fram Strait region via the Transpolar Drift Stream. Finally, the link between the sea-ice export and the North Atlantic Oscillation (NAO) index is briefly discussed. The overall results from this study show that the Arctic Basin and its ice volume anomalies must be considered in order to fully understand the export through Fram Strait.

1 Introduction

In the Arctic region, the presence of the pack ice significantly affects air-sea interactions and influences high-latitude weather and climate. The sea-ice cover reflects a large part of the incoming solar radiation and restricts exchanges of heat, moisture and momentum between the ocean and the atmosphere. In addition, the atmospheric energy budget is highly dependent on the latent heat released during ice formation and the heat absorbed during the melting of ice at high latitudes. Also, salt rejection during ice formation can lead to overturning motions in the ocean and hence affect the ocean thermohaline circulation. In these ways, sea-ice has strong effects on the dynamics and thermodynamics of the atmosphere and ocean, which in turn feed back on the sea-ice and affect its variability on seasonal, interannual and longer time-scales. The main causes of the interannual variability of the sea-ice cover in the Arctic, the main subject of this study, are the year-to-year variations in the atmospheric fields of wind and temperature (Tremblay and Mysak 1998).

Because of the high sensitivity of the Arctic sea-ice cover to atmospheric forcing, this medium can be a good indicator of climate change associated with global warming, which is expected to be amplified in the polar regions (Houghton et al. 1996). In view of this, it is important to understand the dynamic and thermodynamic causes of sea-ice natural variability, in order to separate it out from anthropogenically forced changes.

G. Arfeuille (✉)
Institute of Ocean Sciences, Patricia Bay,
PO Box 6000, Sidney, British Columbia,
Canada V8L 4B2
E-mail: gilles@ocean.seos.uvic.ca

L. A. Mysak
Centre for Climate and Global Change Research
and Department of Atmospheric and Oceanic Sciences,
McGill University, 805 Sherbrooke Street West,
Montreal, Quebec, Canada H3A 2K6

L.-B. Tremblay
Lamont-Doherty Earth Observatory, Columbia University,
Palisades, NY 10964, USA

Our main objective is to obtain a thorough understanding of the role of wind stress forcing in producing anomalous sea-ice export from, and interannual sea-ice cover changes in the Arctic. To achieve this objective, we integrate a thermodynamic-dynamic sea-ice model based on a granular rheology (Tremblay and Mysak 1997) for the (nearly) 41-year period extending from January 1958 to June 1998, and determine the interannual fluctuations in the Arctic sea-ice cover that are solely due to changes in the wind field. Hence, the observed monthly mean wind stresses for the 41-year period are used; all the other atmospheric and oceanic forcings are set to their climatological values.

Another motivation lies in the belief that the recent ocean climate (fresh water) events in the northern North Atlantic known as the 1960s/1970s Great Salinity Anomaly (GSA, Dickson et al. 1988) and the GSAs of the 1980s and 1990s (Belkin et al. 1998) can be due to or influenced by anomalous sea-ice exports from the Arctic Basin into the Greenland Sea via Fram Strait (Mysak et al. 1990; Walsh and Chapman 1990). Since the upper ocean fresh water anomalies can reduce deep water formation in certain regions of the northern North Atlantic (e.g., Labrador Sea), it is important to better understand the strength and frequency of the sea-ice export anomalies through Fram Strait.

This paper build on earlier modelling studies of the interannual variability of the sea-ice cover in the Arctic Basin and its export through Fram Strait. A seminal study in this field is that of Walsh et al. (1985), who pointed out the dominance of thermodynamic processes in producing the annual cycle in the Arctic sea-ice cover, and the dominance of dynamic processes for the interannual fluctuations. Other more recent studies tend to confirm this conclusion. For example, Maslanik and Dunn (1997) showed that the interannual variability in mean ice extent and ice volume is primarily due to the variations in the wind-driven sea-ice transport in the Arctic Basin. These results motivated us to use wind stress forcing as the only year-to-year varying forcing.

Using a coupled sea-ice-ocean model, Häkkinen (1993) established the importance of large-scale wind anomalies over the Arctic Basin in generating ice anomalies. This hypothesis was proposed by Walsh and Chapman (1990) and recently discussed in Mysak and Venegas (1998). Using a cross correlation analysis, Mysak and Power (1992) showed that ice concentration anomalies formed in the Beaufort Sea can propagate into the Greenland Sea in about two to three years. This result is also consistent with the model results obtained by Tremblay and Mysak (1998), who showed that sea-ice thickness anomalies formed in Beaufort-Chukchi Sea can be advected anticyclonally around the Arctic Basin and then exported out of the Arctic through Fram Strait.

The sea-ice model is briefly described in Sect. 2. The forcing data used for the simulations are described in Sect. 3, and a description of the experiments run is given in Sect. 4. In order to validate the results of the 41-year

run, the Fram Strait sea-ice export results are first compared with model results from another numerical study (Häkkinen 1995) for the 1960–85 period (in Sect. 5); the model results are also compared with measured sea-ice export in the Fram Strait region during the 1990–96 period (Vinje et al. 1998). In Sect. 6, we analyze the structure of the interannual variability of the sea-ice export through Fram Strait, with a particular focus on the sea-ice thickness and velocity contributions to the year-to-year variations. The relation between the sea-ice export through Fram Strait and the origin of the GSA of the 1960s/1970s is investigated in order to quantify the Arctic sea-ice contribution to the fresh water outflow in the northern North Atlantic. In Sect. 7 the outflow is related to events in the Arctic basin itself, especially to sea-ice volume anomalies in the Arctic basin for the 41-year period 1958–98. The origin of these sea-ice volume anomalies and their space time evolution in the Arctic Basin are then described and related to the atmospheric forcing field. In Sect. 8 the relation between the sea-ice export and the North Atlantic Oscillation is briefly explored. A summary of the results is given in Sect. 9.

2 Sea-ice model

The domain over which the sea-ice model is integrated in the present work includes the Arctic Ocean and surrounding seas (see Tremblay and Mysak 1998). The sea-ice in the model is assumed to behave as a granular material in slow continuous deformation under the action of the winds and ocean currents. This is motivated by observations of the Arctic sea-ice cover which show a distinct lead pattern at various scales that is typical for that type of material (Erlingsson 1988). This type of model has also been successfully applied to the deformation of other materials showing similar deformation patterns as in sea-ice (e.g. sand, land slides, etc.). The present approach differs from the standard Hibler model (Hibler 1979) in the way the internal ice pressure is calculated, and in the choice of the yield curve and flow rule. A formal comparison between these two models is under way (L.-B. Tremblay, personal communication). In the present model, the resistance of sea-ice to compressive load is considered to be a function of its thickness and concentration, and its shear resistance is proportional to the internal ice pressure at a point. In divergent motion, the ice offers no resistance and the floes drift freely. The boundary conditions for the ice dynamic equations are zero normal and tangential velocity at a solid boundary and free outflow at an open boundary. The sea-ice model is coupled thermodynamically with a mixed layer ocean model, in which the temperature and salinity at open boundaries are specified from monthly climatologies extracted from Levitus (1994). At continental boundaries, the ocean heat flux is considered to be zero (a continent is regarded as a perfect insulator). A detailed description of the dynamic and thermodynamic components of the ice model can be found in Tremblay and Mysak (1997).

3 Atmospheric and oceanic forcing data

The model was forced with monthly mean wind stresses obtained from over 40 years (January 1958 to June 1998) NCEP Reanalysis daily averaged sea level pressure (SLP), and climatological monthly mean air temperatures obtained from the NCEP Reanalysis daily 2-m air temperature. The SLP includes the International Arctic Buoy Program (IABP) drifting buoy data since the time they have

been available. The NCEP Reanalysis data are produced in collaboration with the National Center for Atmospheric Research (NCAR). For more information on the NCEP data, see Kalnay et al. (1996). For the ocean, the temperatures at the southern part of the Greenland Sea were specified from monthly climatologies extracted from Levitus (1994). The ocean currents were spatially varying but steady (annual mean values, since the goal of this study is to focus on the effects of the wind); they were obtained using a single-layer reduced gravity model appropriate for large-scale flow (Tremblay and Mysak 1997). Levitus sea surface elevation data were used to specify the inflow/outflow velocity field in the northern North Atlantic; the latter was scaled in such a way as to obtain no accumulation of water in the Arctic domain (Tremblay and Mysak 1997). The normal component of the velocity in Bering Strait was chosen so as to obtain a constant inflow of 1 Sv into the Arctic Ocean.

The values of the physical parameters used in this study are comparable to those used in other ice modelling studies (e.g., Hibler 1979). They were chosen to obtain consistency with the estimated mean ice thickness over the Arctic domain (Aagaard and Carmack 1989), and with the observed mean ice velocity and thickness in the Fram Strait region (Vinje et al. 1998). The resulting mean sea-ice export, however, is somewhat larger than observed since in the model the full width of Fram Strait is covered by sea-ice (in reality, the West Spitsbergen Current keeps the eastern part of the channel free of ice).

4 Spin-up and simulation

The initial conditions for this study were obtained from a 20-year run forced with climatological data in order to reach a stable periodic seasonal cycle, followed by a four-year run forced with monthly varying NMC data extending from 1954–57. The latter allowed us to start the 41-year run (i.e., January 1958 to June 1998) with more appropriate initial conditions. The NCEP Reanalysis data set was used to compute the climatological monthly mean temperature, using data from the 40-year period 1958–97. The simulations were performed with a one-day time step. The monthly mean forcing fields are considered to represent mid-month values. The daily values of the forcing fields were obtained by the weighted average of the two closest mid-month values. Since only the wind stress forcing varies from year to year in the 41-year run, the simulated sea-ice interannual variability presented in the next sections is mainly due to dynamic processes.

5 Comparison of Fram Strait sea-ice export with other model results and observations

The sea-ice transport out of the Arctic Basin is an important quantity to consider. Most of this transport is through Fram Strait. According to Alekseev et al. (1997), less than 5% of the total passes through the Canadian Arctic Archipelago and less than 1% exits via the Barents Sea. However, recently Melling (1999) estimated that up to 20% of this transport could be through the Archipelago. Mauritzen and Häkkinen (1997), using a fully prognostic coupled ocean-ice model, showed the significant role played by the sea-ice export through Fram Strait in determining the strength of the thermohaline circulation in the North Atlantic Ocean.

In order to determine whether the anomalies of the sea-ice export through Fram Strait are realistic, a comparison was first made with earlier model results (Häk-

kinen 1995). Häkkinen (1995) produced a 26-year Arctic ice-cover run (1960–85) using daily winds as forcing. For the overlapping period (1960–85), the sea-ice export anomaly peaks found in the two studies correspond very well, and the amplitudes of the departures from the mean are comparable (see Fig. 1a).

The simulation results were also compared with observed sea-ice export through Fram Strait for the six-year period from August 1990 to August 1996 (Vinje et al. 1998). During this six-year period the sea-ice thickness and velocity in Fram Strait were measured, and from these the mean ice export was computed to be 2875 km³/y. This value is in agreement with the 2800 km³/y export estimated by Aagaard and Carmack (1989). To make the sea-ice export anomaly comparison between the observations and our results, the model mean sea-ice export over the 41-year period (just over 5000 km³/y) was subtracted from the model sea-ice export obtained during this six-year period to obtain the model anomaly export for this recent period. (It should be noted that because the simple ocean model used in this study does not include the West Spitsbergen Current, WSC, the simulated sea-ice export through Fram Strait is larger than observed. The relatively warm

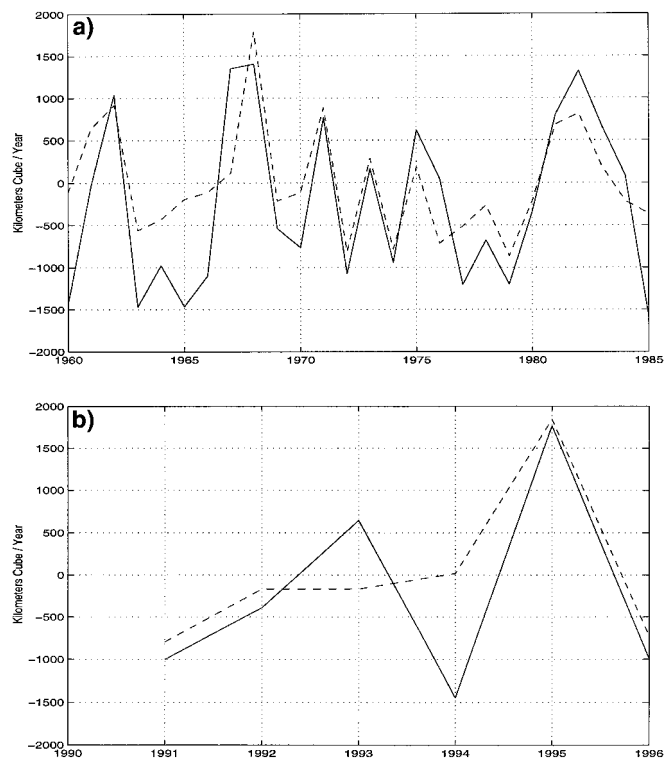


Fig. 1 a Comparison of anomalies of sea-ice export through Fram Strait in km³/year: results from our 41-year run (solid line) versus those from the Häkkinen (1995) 26-year run (dashed line). b Sea-ice export anomaly through Fram Strait in km³/y from August 1990 to August 1996: model results (solid line) versus Vinje et al. (1998) observations (dashed line). Note: a data point for a given year is the average of the monthly anomalies from August of the previous year to July of the given year

northward WSC is responsible for melting part of the outflowing sea-ice in the Fram Strait region.) The model anomaly was compared with the observed sea-ice export anomaly obtained by subtracting the observed mean sea-ice export over the six-year period (1990–96) from the observed sea-ice export.

Figure 1b shows that the model and observed departures for the six-year period have the same order of magnitude. The slope of the increasing export during the first year of the observations is the same as in the model results. The largest observed export anomaly occurs during the period from August 1994 to July 1995 and is well represented in the model results. This large export anomaly of $1760 \text{ km}^3/\text{y}$ is the second largest in the simulation during the 41-year period 1958–98. While the observations show a plateau for the period from August 1992 to July 1994, the model gives two compensating peaks giving a mean that corresponds to the observed value. It should be noted that in the model results for the period from August 1992 to July 1993, the sea-ice is a little thicker than observed, and for the period from August 1993 to July 1994 the sea-ice velocity is a little smaller than observed (not shown here). However, the results obtained by Kwok and Rothrock (1999) (not shown here) using satellite microwave data show a local minima during the period from August 1993 to July 1994, which confirms our results.

It is important to recall that in the simulation, the air temperature does not vary from year to year. Also, the effects of the variability in the strength of the WSC and the variability of heat transported by it (Hibler and Walsh 1982) are not included in the model, and these have an effect on the width of the ice stream in the Fram Strait region (and therefore also on the ice export). Also, the use of monthly mean wind data tends to smooth the year-to-year fluctuations in the sea-ice export; however, since the simulated width of the ice stream in Fram Strait is larger, the resulting amplitude of the ice export anomalies are of the same order of magnitude as the observed ones. Therefore, we regard the modelled sea-ice export anomalies as being representative of the observed sea-ice export anomalies since the results reproduce the magnitude and timing of the large observed sea-ice export anomalies in 1994–95, despite the use of monthly mean wind stress forcing. Moreover, our anomaly results correspond well with those obtained using a model which includes a more complex ocean (Häkkinen 1995).

6 Analysis of the interannual variability of the sea-ice export through Fram Strait

6.1 Major export anomaly events

The model sea-ice export time series through Fram Strait shows five large ($> 1000 \text{ km}^3/\text{y}$) positive anomalies during the 41-year period: 1959, 1967–68, 1981–83,

1989, and 1995 (Fig. 2). The second, third and fourth anomalies are preceded by periods of large negative anomalies. As will be seen in Sect. 7, during these latter periods there are increases in the sea-ice volume in the Arctic Basin.

The 1967–68 sea-ice export anomaly is considered to be the origin of the GSA of the late 1960s/1970s. To explain the presence of the salt deficit and negative sea surface temperature anomalies in the Iceland Sea in 1968, Belkin et al. (1998) argued that a positive anomaly in sea-ice export through Fram Strait should start at least during the second part of 1967. This is in agreement with the modelled results which show two large exports in 1967 and 1968 (see Fig. 2).

The results of the 41-year run show an anomaly of 1353 km^3 during the second half 1967, another one of 1405 km^3 during the first half 1968, and very small contributions during the first half of 1967 and second half of 1968. When averaged over the two-year period 1967–68, this gives a mean anomaly of just under $1500 \text{ km}^3/\text{year}$ (Fig. 2). For the period from August 1967 to August 1968 the total amount of excess sea-ice export is 2758 km^3 . Mauritzen and Häkkinen (1997) showed that around 40% of the Fram Strait sea-ice export is transported through Denmark Strait and further to the Labrador Sea and the subpolar gyre. In this simulation, 40% of the total excess of 2758 km^3 in sea-ice export yields a value of 1103 km^3 . This is more than the half of the 2000 km^3 of fresh water excess in the Labrador Sea estimated by Dickson et al. (1988) to explain the salt deficit there at the beginning of the 1970s. Also, other significant export anomalies occurring during the 1967–68 period but not considered here could contribute to the fresh water anomaly in Labrador Sea (e.g., Canadian Arctic Archipelago throughflow, the outflow from the Arctic Ocean in the mixed layer). Therefore, the excess of sea-ice export through Fram Strait during the 1967–68 period can explain a large part of the negative salinity anomaly in Labrador Sea during the 1969–70 period and hence could be part of the origin of the GSA of the 1970s.

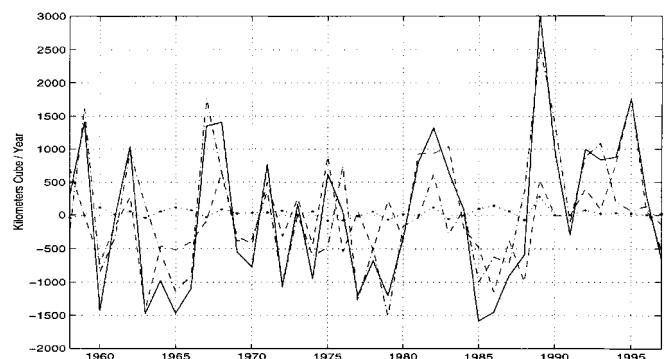


Fig. 2 The sea-ice export anomaly through Fram Strait in km^3/y (solid line) decomposed (to within a constant) into $h'v'$ (dotted line), $v'h$ (dashed line), $h'v - \bar{h'v}$ (dash-dotted line), and $(h'v - \bar{h'v})$ (a negligibly small contribution of 0 ($20 \text{ km}^3/\text{y}$) not shown here)

6.2 Contribution of the sea-ice thickness anomalies to the sea-ice export anomalies

The sea-ice export (transport) through Fram Strait is proportional to the product of the sea-ice thickness and velocity in the Fram Strait region. It can be expressed in terms of the mean values and anomalies of the sea-ice thickness (\bar{h} and h') and sea-ice velocity (\bar{v} and v') in the Fram Strait region as (to within a constant proportional to the width of the Fram Strait):

$$hv = \bar{h}\bar{v} + (hv)' = \bar{h}\bar{v} + h'\bar{v} + v'\bar{h} + h'v'. \quad (1)$$

From Eq. (1) it follows that the sea-ice export anomaly can be written as

$$(hv)' = (\bar{h}\bar{v} - \bar{h}\bar{v}) + h'\bar{v} + v'\bar{h} + h'v'. \quad (2)$$

Figure 2 shows the three main contributions to the sea-ice export anomaly. The term in parentheses in Eq. (2) is negligibly small (less than 1% of the observed mean sea-ice export) and is not plotted in the figure.

From these results, we first note that the product $h'v'$ is not a significant component of the export (i.e., h' and v' are not correlated: the product $h'v'$ is sometimes positive and sometimes negative). Therefore, there is no direct relation between the sea-ice thickness anomaly and velocity anomaly in the Fram Strait region. The two other contributions in this decomposition indicate that for the large sea-ice export anomalies in 1959, 1967–68, and 1989, the positive anomaly in the ice export was mainly due to thicker than usual sea-ice. This result is in agreement with that obtained by Häkkinen (1993) for the 1967–68 event (the other years were not included in the Häkkinen simulation).

In Fig. 3 we compare the northerly wind stress anomalies in Fram Strait (normalized by the maximum value) with the normalized sea-ice export anomaly for the 41-year integration period. From this figure and Fig. 2 it is clear that the northerly wind in Fram Strait is not necessarily the dominant factor in producing anomalies of sea-ice export. For example, during the 1967–68 large export period, the northerly wind stress anomaly only became

larger in 1968, in the second year of this large export period, and thus played an important role in the export in 1968 only. This is confirmed by the large contribution of the $v'h$ term to $(hv)'$ in 1968 (Fig. 2); the large contribution of the $h'\bar{v}$ term in 1967 indicates that, the large export in that year was due to the thickness anomaly. The dominance of the thickness anomaly is especially true for the sea-ice export anomaly in 1989, which is the largest anomaly of the whole 1958–98 period. This large sea-ice export is due to very thick ice being exported out of the Arctic Basin (see $h'\bar{v}$ curve in Fig. 2).

In contrast, the sea-ice export anomaly in 1995, (second largest in the 41-year run), is due to an anomaly in the sea-ice velocity (see $v'h$ curve in Fig. 2). This is consistent with the observations made by Vinje et al. (1998) and with the large 1995 peak in the northerly wind stress (see Fig. 3). Both observations and model results show that the 1990–96 large export events were mainly due to the wind anomalies; this led Vinje et al. (1998) to conclude that the wind anomalies in the Fram Strait region are the main cause of large sea-ice export anomalies through Fram Strait. Also, many earlier studies (Alekseev et al. 1997) considered the northerly wind in the Fram Strait region to be the main driving mechanism for the sea-ice export. Generally, the normalized northerly wind anomalies and the normalized sea-ice export anomalies, while coincident in time, are not comparable in magnitude. Alekseev et al. (1997) and Smirnov and Smirnov (1998) used statistical data-based models to estimate the sea-ice export through Fram Strait relating the pressure gradient across the Strait to the sea-ice export by a linear relation. The years covered by the observations show a very high correlation between the two quantities, but the observed export data is quite sparse in time; also, this approach totally neglects the evolution of the sea-ice in the Arctic.

Anomalous wind patterns over the Arctic Basin can produce anomalous sea-ice extent and thickness anomalies there. These sea-ice anomalies can be advected all along the basin (Tremblay and Mysak 1998) and can affect the sea-ice dynamic behavior. This and the preceding results show the importance of knowing the sea-ice thickness distribution and circulation pattern inside the Arctic Basin before it is exported through Fram Strait, a feature pointed out by Walsh and Chapman (1990). The relation between the anomalies in sea-ice export through Fram Strait and the prior volume anomalies in the Arctic Basin will be discussed in the next section. The link between the volume anomalies and atmospheric patterns in the Arctic Basin will then be described.

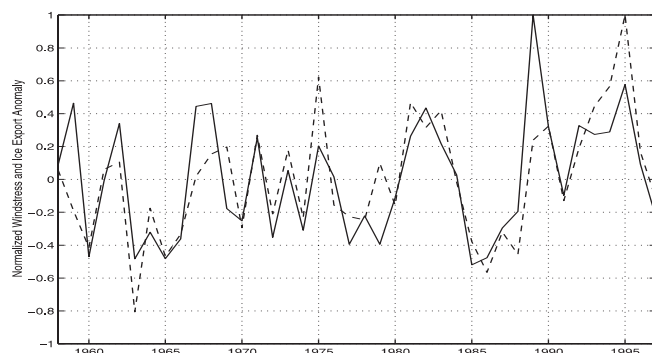


Fig. 3 Normalized northerly wind stress anomaly in Fram Strait region (dashed line) versus normalized sea-ice export anomaly through Fram Strait (solid line). The wind stress and ice export anomalies are normalized by their respective maximum values

7 Interannual variability of the sea-ice volume in the Arctic Basin and its relation to atmospheric forcing

The results in the previous section show that sea-ice thickness anomalies are an important contributor to anomalous sea-ice export through Fram Strait. For this

reason it is important to consider the evolution of the sea-ice cover in the Arctic Basin. Walsh and Chapman (1990) pointed out that the variability in the pressure difference between southern Greenland and the Arctic-Asian coast corresponds well with the large sea-ice export in the 1960s. They concluded that thicker (multi-year) ice from the Arctic Basin could be advected into the Fram Strait region and contribute to a larger sea-ice export. The results of the previous section (see Fig. 2) confirm this conclusion. Therefore, we first want to consider ice volume anomalies in the Arctic Basin. Secondly, by dividing the Basin into nine regions, we can determine the origin and the propagation of each of the sea-ice volume anomalies. Lastly, we search for the atmospheric patterns which created them and help drive them through the Arctic Basin toward Fram Strait.

7.1 Sea-ice volume anomalies

The sea-ice volume and extent were computed from the model results. A mean sea-ice thickness of 3.1 m and a mean sea-ice extent of $6.7 \times 10^6 \text{ km}^2$ over the 41-year period were obtained. These values are in good agreement with the estimates by Aagaard and Carmack (1989) (3-m mean ice thickness), and by Parkinson et al. (1987) ($6.5 \times 10^6 \text{ km}^2$ sea-ice extent). Thus, the computed mean ice volume is $2.08 \times 10^4 \text{ km}^3$. The annual mean sea-ice volume anomalies for the Arctic Basin are computed for the 41-year period and compared with the sea-ice export anomaly through Fram Strait (see Fig. 4). The two quantities are comparable in magnitude. In addition, Fig. 4 suggests that there may be a lag between the two quantities, with large ice export events following large volume anomalies by about two years.

In order to analyze the evolution of the Arctic Ocean sea-ice volume anomalies, the Arctic Basin is divided into nine regions (see Fig. 5): 1: Beaufort Sea; 2: Chukchi Sea; 3: East Siberian Sea; 4: eastern Arctic; 5: Laptev Sea; 6: central Arctic; 7: Canadian Basin; 8: north of Fram Strait, and 9: Kara and Barents Seas. At first the basin was divided into four quarters, and then the nine

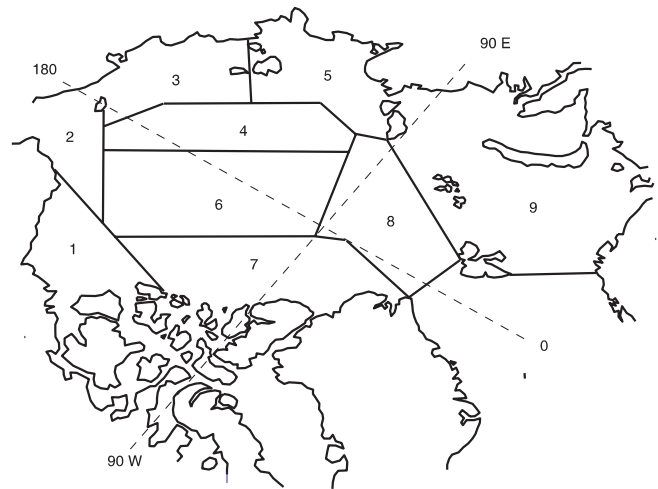


Fig. 5 The Arctic Basin divided into nine regions

regions defined were chosen according to the variability of the sea-ice volume anomalies in these four quarters. The sea-ice volume anomaly was then computed for each region (see Fig. 6). It should be noted that the sea-ice volume anomalies in the Kara and Barents Seas region are not plotted since the sea-ice volume anomalies were insignificant there.

The Beaufort Sea has a relatively large ice volume anomaly in 1964–65 (in agreement with Tremblay and Mysak 1998), but only a small part of it is transported through to the Chukchi Sea (see Fig. 6a, b). However, a sea-ice volume anomaly later starts to really increase in the East Siberian Sea in 1965 (Fig. 6c) and can be found later in the eastern Arctic (Fig. 6d) (the lag is more evident for the other periods studied). This anomaly is believed to be only partly advected from the Chukchi Sea; it is mainly formed locally in the East Siberian Sea (see next section). It persists as a smaller anomaly in the Laptev Sea (Fig. 6e) and then gets stronger and appears later in the central Arctic (Fig. 6f), and then north of Fram Strait (Fig. 6h) and in the Canadian Basin region (Fig. 6g), before being exported through Fram Strait in 1967, which is a year of large export due to thick ice (Fig. 2). For the late 1960s period, Serreze et al. (1992) concluded that the multi-year sea-ice could come from along the northern coasts of Greenland and Ellesmere Island where the sea-ice is very thick (up to 7 or 8 m) due to packing along this coastline. The 1967 sea-ice volume anomaly in region 7 is 400 km^3 . To verify whether this anomaly would contribute to the sea-ice export through Fram Strait, this region was divided into two bands, one adjacent to the coast and another to the north of the first band. It was then found that the anomaly was effectively transported to north of Fram Strait from the band that was farther away from the coast, and thus was not coming from immediately north of Greenland.

In 1973 and 1974, an anomaly starts to grow in the Beaufort Sea, but a season-by-season analysis of the results (not shown here) showed that this sea-ice volume

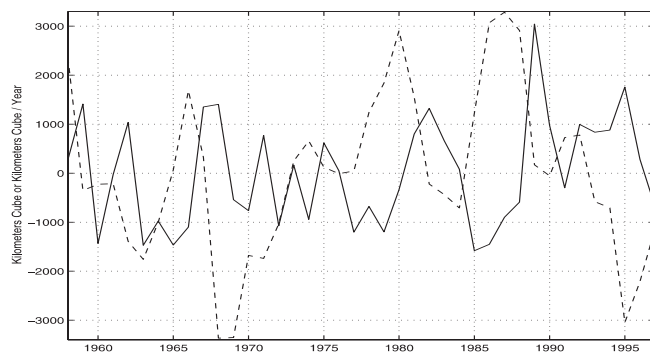


Fig. 4 Annual mean sea-ice volume anomaly in the Arctic Basin (dashed line) in km^3 versus sea-ice export anomaly through Fram Strait (solid line) in km^3/y

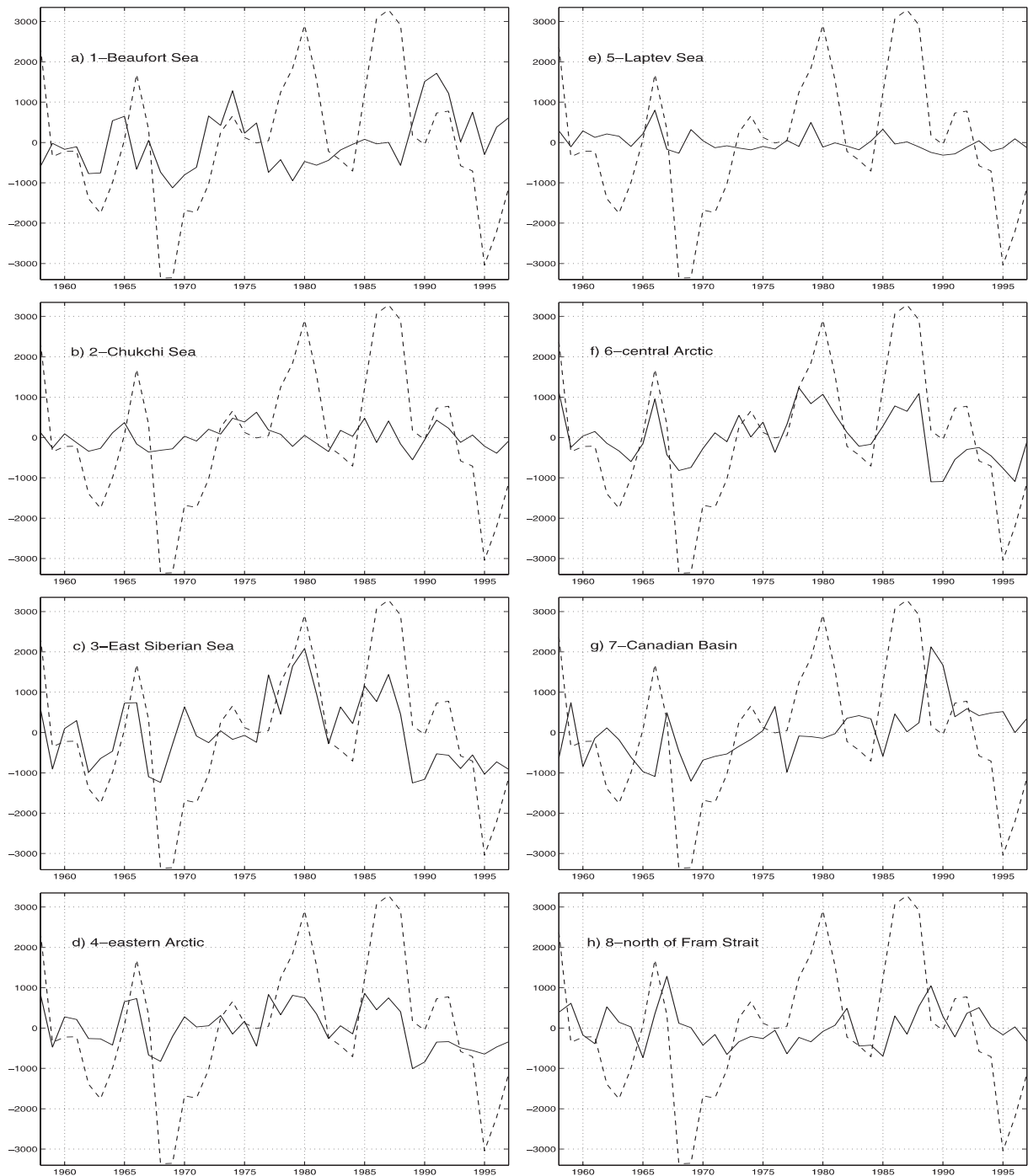


Fig. 6a–h Sea-ice volume anomalies in km^3 for eight of the regions (*solid lines*) and for the whole Arctic Basin (*dashed line*): **a** 1-Beaufort Sea, **b** 2-Chukchi Sea, **c** 3-East Siberian Sea, **d** 4-eastern Arctic, **e** 5-Laptev Sea, **f** 6-central Arctic, **g** 7-Canadian Basin, and **h** 8-north of Fram Strait

anomaly remained a local anomaly, and disappeared at the end of 1975.

A very small sea-ice volume anomaly which formed during the summer of 1976 in the Beaufort Sea (Fig. 6a) seems to have been partly transported to the Chukchi Sea (Fig. 6b), and then to the East Siberian Sea (Fig. 6c), where it increases substantially due to the local wind anomaly in East Siberian Sea. The large sea ice volume anomaly in the East Siberian Sea (Fig. 6c) which

appears during the 1978–81 period (2000 km^3) was not completely transported to the whole central Arctic (regions 4 and 6); it seems to have remained a more local feature since only a little more than two-thirds of the anomaly can be found in this region (Fig. 6d and f). However, only a part of the latter anomaly was transported from the central Arctic to the north of Fram Strait during the 1978–81 period and then exported through Fram Strait.

For the 1984–89 period, the anomalies really start to form and increase first in the East Siberian Sea and then in eastern Arctic, where they grow earlier than the central Arctic volume anomalies. In the eastern Arctic, the sea-ice volume anomaly starts to grow in 1984–85 followed by an increase in the ice volume anomaly in the central Arctic (region 6, Fig. 6f) in 1986. The ice volume anomalies peak up in the Canadian Basin region and north of Fram Strait (see Fig. 6g, h) during the export periods, when at the same time, they are decreasing in the whole central Arctic (Fig. 6d and f). For the peak in the Canadian Basin region in 1989, the aforementioned subarea study (two bands) shows that the sea-ice volume anomaly comes effectively from the coast and does not appear in the northernmost band; it goes directly to the north of Fram Strait before it is exported through Fram Strait. Therefore, multi-year sea-ice formed along the coast of Greenland and Canadian Archipelago can be

advected through Fram Strait, which is the case in 1989, but this did not seem to be the case during the 1967–68 period, as proposed by Serreze et al. (1992).

For the large volume anomaly periods (1965–67, 1977–81, and 1985–89) preceding the large export periods, the anticyclonic circulation of the ice volume anomalies described can be generally viewed as typical of the formation of sea-ice volume anomalies in the East Siberian Sea. An example of this anticyclonic circulation is shown in Fig. 7 for the 1984–89 period. The corresponding atmospheric circulation patterns causing this type of circulation are described in the next section. It should be noted that the sea-ice volume anomaly north of Fram Strait is smaller than the export anomaly for the periods where the large sea-ice export is due to an anomaly in the sea-ice velocity (see Figs. 2, and 6h). In this region the circulation increases, and there is no substantial accumulation of sea-ice north of Fram Strait

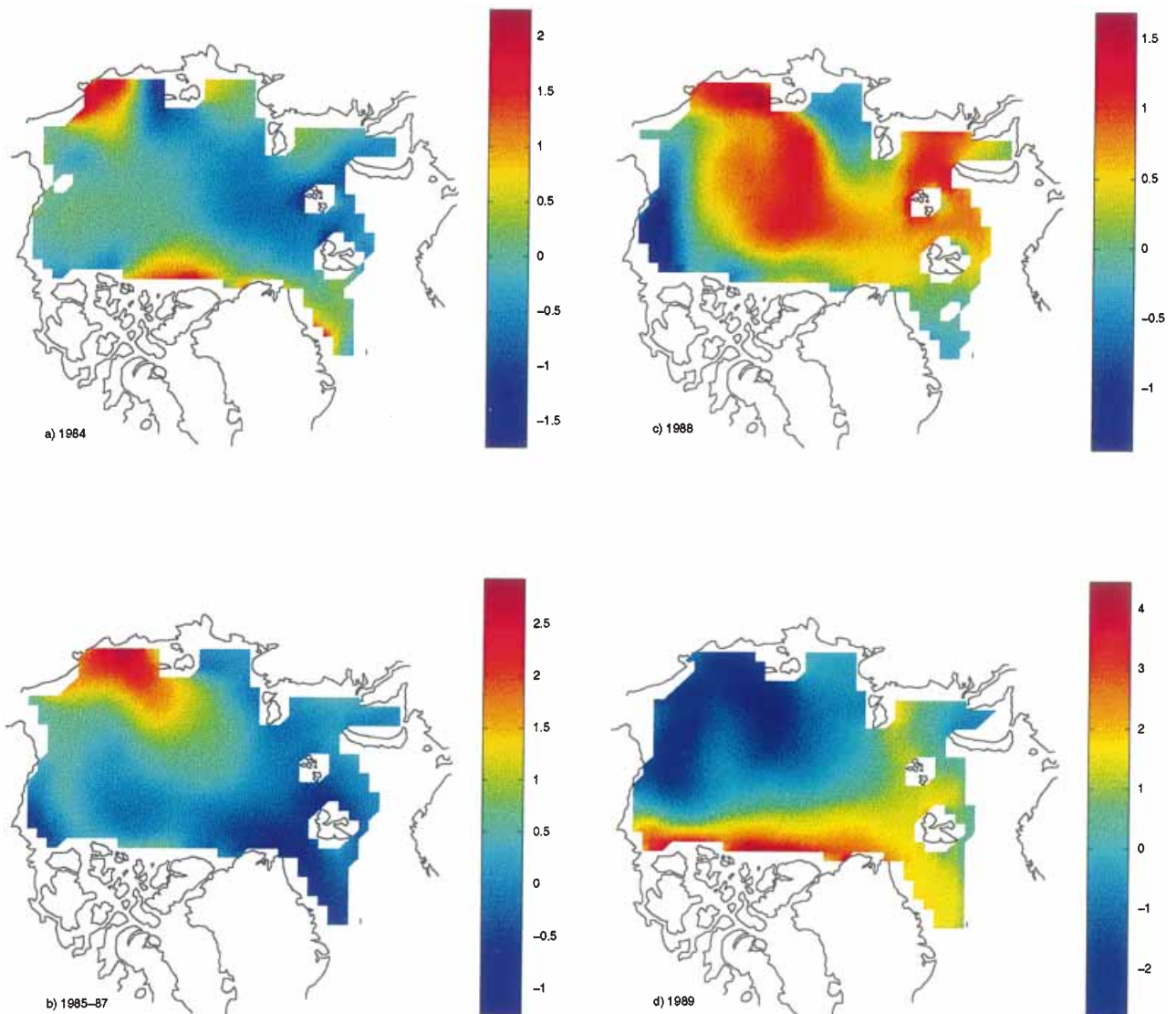


Fig. 7 Sea-ice volume anomalies for the 6-year period 1984–89. Thickness scales to the *right* of each figure are in meters, and each color bar has a different scale

(during the 1981–83 period and especially during the 1994–95 period). For the years of large export due to an anomaly in thickness, the sea-ice volume anomaly is visible (i.e., in 1967 and 1989). For the large sea-ice export during 1967–68, when the anomaly was due to the change in sea-ice velocity ($\bar{v}h$ term) and reached its maximum value in 1968, there was no more accumulation of sea-ice and the sea-ice volume anomaly decreases rapidly even though the export still had a large value.

These results describing the anticyclonic circulation of the anomalies in the Arctic Basin agree with the model results obtained by Tremblay and Mysak (1998) who showed that an ice thickness anomaly formed in the Beaufort Sea could be transported around the basin with the same anticyclonic circulation and the same time scale. These results are also consistent with Mysak and Venegas (1998) who used a combined complex orthogonal function analysis to show the anticyclonic propagation of sea-ice concentration anomalies in the Arctic Basin and their export through Fram Strait into the Greenland Sea.

7.2 Sea level pressure patterns and their relation to the sea-ice circulation

A further understanding of the results can be obtained by examining the sea-level pressure patterns from the NCEP Reanalysis Data set and the sea-ice velocity fields obtained from the model for the ice volume change periods 1964–66, 1978–80, 1985–88, 1991–93 (see Figs. 8–11 a, b, and c), and the subsequent large export periods 1967–68, 1981–83, 1989, and 1994–95 (see Figs. 8–11 d, e, and f).

The mean sea-level pressure (SLP) fields for these short periods were computed from the monthly data (see parts a or d in Figs. 8–11). The anomalous mean sea-ice velocity fields were computed by subtracting the climatological sea-ice velocity field (from the 41-year run) from the mean sea-ice velocity fields for the same period to yield anomaly fields (see Figs. 8–11 b or e). The anomalies in the SLP fields (see in Figs. 8–11 c or f) were also computed for these periods by subtracting the mean of the 41-year SLP record from the mean SLP over the corresponding period.

The anomalies in the sea-ice velocity field show that for the three periods of large and/or increasing sea-ice volume in the Arctic Basin (1964–66, 1978–80, and 1985–88) which occurred before a large export, the circulation tends to pack the ice along the East Siberian coast more than usual (see Figs. 8–10 b). Since it is in this region that the volume anomalies in the Arctic Basin start to grow (Fig. 6c), the origin of this increase is the packing of the ice along the coast of East Siberia. It is remarkable that during these periods of volume increase, the high pressure system over the Arctic Basin (the Arctic High) is centered closer to the Asian continent with isobars showing a geostrophic wind which pushes the ice toward the coast (see Figs. 8–10 a). The SLP

anomalies (Figs. 8–10 c) show a higher than usual SLP along the East Siberian Coast; this is consistent with the statement regarding the Arctic High center being near the East Siberian Coast. At this time the Icelandic Low does not extend as far north in the eastern Arctic (see Figs. 8–10 a). This also agrees well with the results obtained by Gudkovich (1961) who compared the atmospheric pressure distribution with the observed sea-ice drift in the Arctic Basin (these results are also reported in Proshutinsky and Johnson 1997). Gudkovich (1961) showed that two types of sea-ice circulation exist in the Arctic Basin: (1) the cyclonic circulation in the eastern Arctic with a small Arctic High centered over the Beaufort Sea (years of large export; see later), and (2) a larger anticyclonic circulation over the whole Basin, with the Beaufort High closer to the Siberian coast, which the authors call the Siberian High (northern extension of the Asian High located over Siberia). In the latter case, the Transpolar Drift Stream slows down and shifts toward North America, leading to cyclonic sea-ice circulation in the East Siberian Sea. Gudkovich (1961) reports that at such a time the navigation conditions are favorable in the Kara Sea but especially unfavorable in the Laptev Sea and East Siberian Sea because these atmospheric conditions lead to packing of the sea-ice along the coast there.

It is interesting to note that the anomalies in the sea-ice velocity fields (see Figs. 8–11 b and e) follow the isobars of the SLP anomalies (see Figs. 8–11 c and f) of the forcing fields. Also, only during the 1964–66 period is there a piling-up of ice in the Laptev Sea (see Fig. 6e). The sea-ice velocity anomalies (see Fig. 8b) tend to pack more of the ice than usual in this region. The Laptev Sea plays a large role in the Arctic as a source of first-year sea-ice; it is a polynya which does not store the sea-ice but produces it (Kassens et al. 1997), right at the tail of the Transpolar Drift Stream. It was mentioned above that during the 1978–81 period, the ice volume anomaly in the Arctic Basin did not propagate as much as the volume anomalies during the other periods. The sea-ice velocity anomalies (see Fig. 9b, and e) show that the ice packing along the coast was quite large, and that during the export period (1981–83) this anomaly is persistent in reducing ice export out of the East Siberian Sea by the Transpolar Drift Stream until 1982.

For the periods of large export anomalies (1967–68, 1981–83, 1989, and 1994–95), the sea-ice anomaly velocity fields (see Figs. 8–11 e) confirm that the circulation tends to transport more ice from the center of the Arctic Basin (where the bulk of the volume anomalies are located) to the Fram Strait region. The SLP patterns show a configuration of the isobars which allows a strong Transpolar Drift Stream, i.e., isobars going from the Laptev Sea to the Fram Strait region quite directly, with in general a strong lateral gradient in Fram Strait Region (see Figs. 8–11 d). This is in agreement with the results in the sea-ice velocity fields showing a well-developed Transpolar Drift Stream for periods of large export (not shown here). The SLP patterns also show

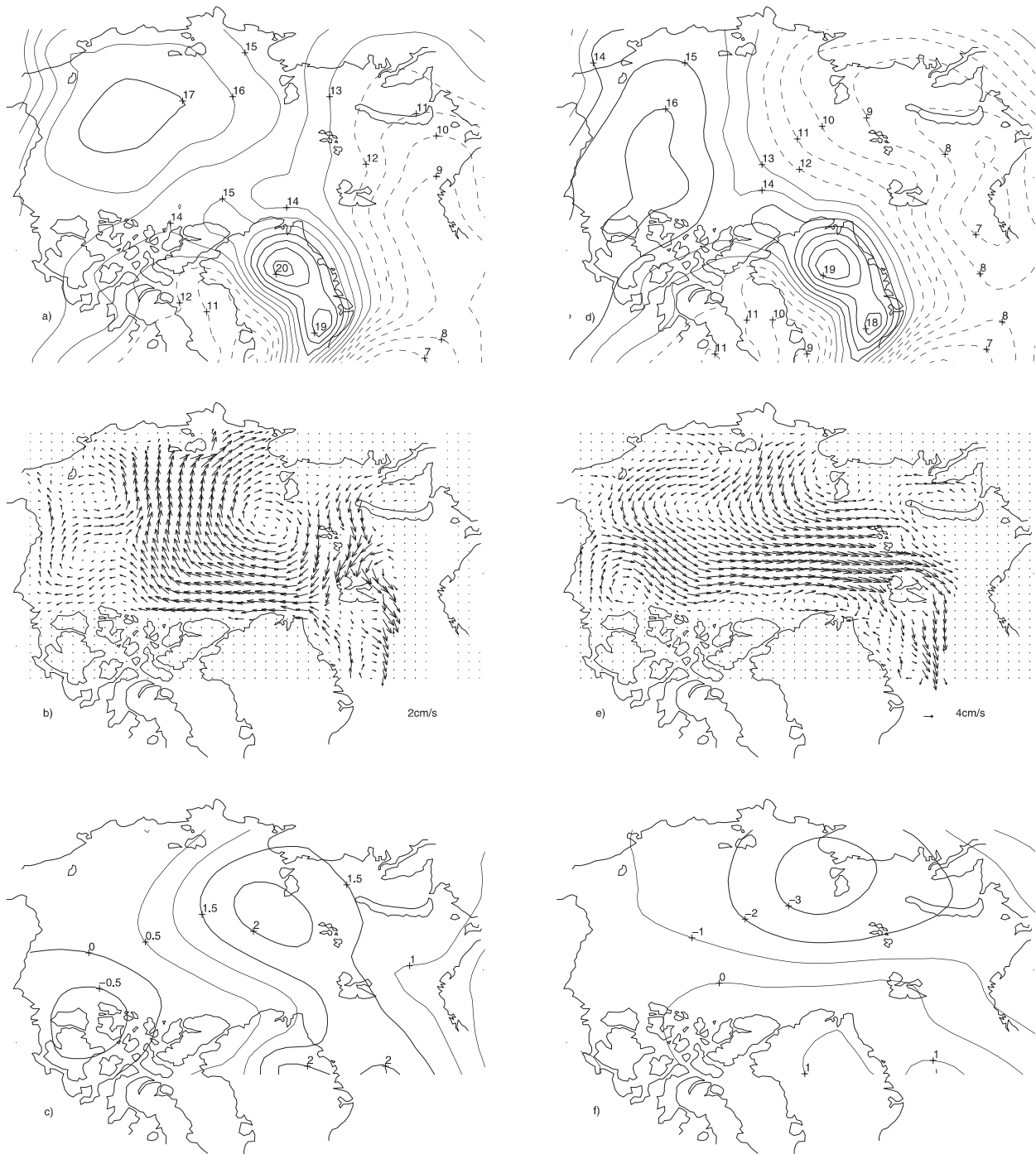


Fig. 8a–f Mean sea-level pressure in hPa (relative to 1000 hPa with SLP contours less than 1013 hPa in *dashed lines*), anomaly in the mean sea-ice velocity field, and anomaly in the mean sea-level pressure field in hPa for the **a–c** 1964–66 period, and **d–f** 1967–68 period

that these periods of large export correspond to an Icelandic Low extending farther than normal into the Arctic Basin, corresponding well with the retreat of the Arctic High, to the southern part of the Beaufort Sea.

The anomalies in the sea-ice velocity field for the 1967–68 period (see Fig. 8e) show that the export of the thick ice next to the coast of Greenland and the Canadian Archipelago was not possible since the anomalous

sea-ice circulation (as the climatology) was extremely weak there. This is due to the presence of the pocket-shape made by the 1015-hPa isobar north of Ellesmere Island (Fig. 8d). The situation was different in 1989, when there was a stronger sea-ice circulation along the coast, which allows the ice to leave the coast and then go to the Fram Strait region (see Fig. 10e).

We pointed out earlier that the large export in 1995 was not preceded by a large increase of volume in the

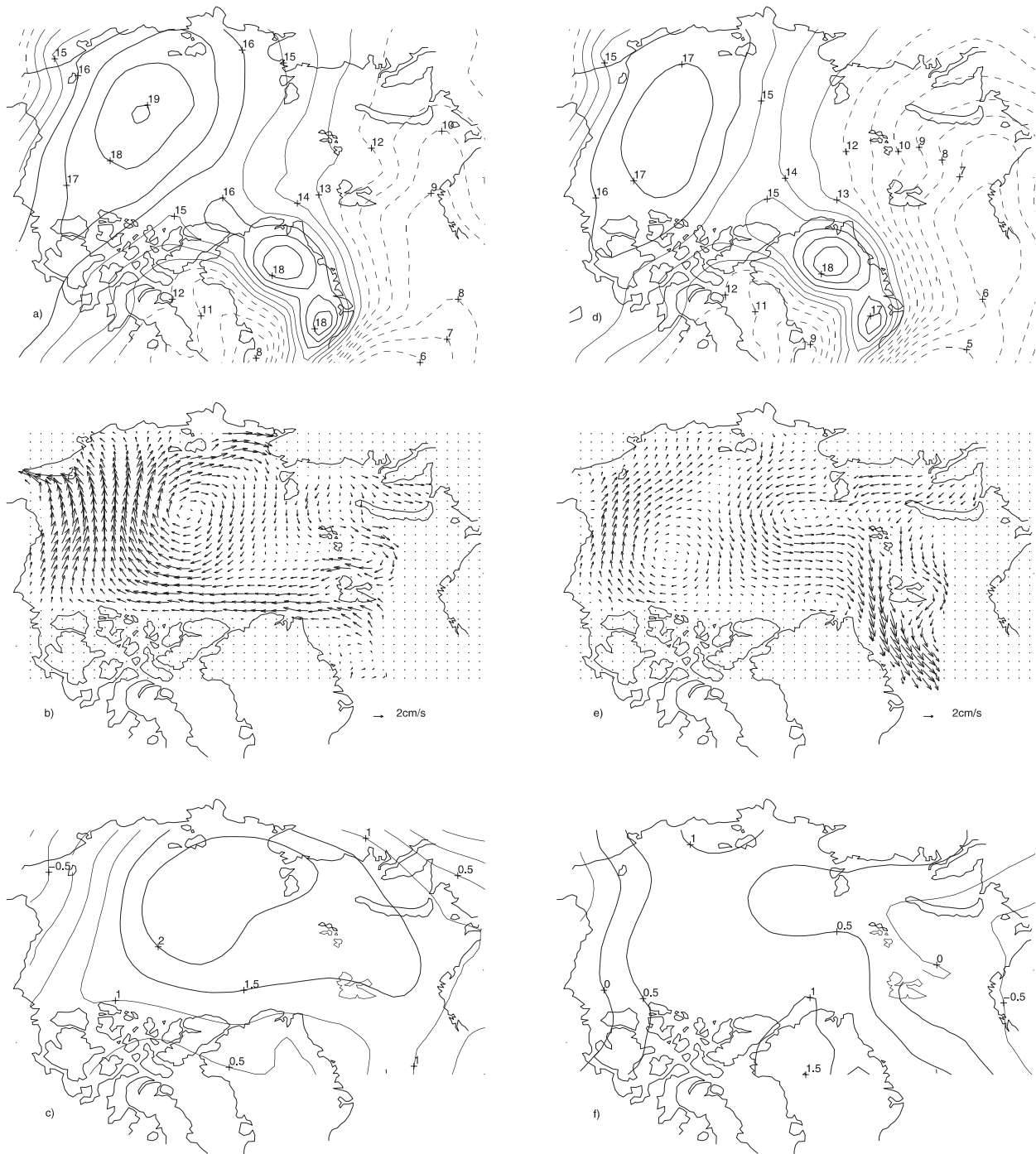


Fig. 9a–f Mean sea-level pressure in hPa (relative to 1000 hPa with SLP contours less than 1013 hPa in *dashed lines*), anomaly in the mean sea-ice velocity field, and anomaly in the mean sea-level pressure field in hPa for the **a–c** 1978–80 period, and **d–f** 1981–83 period

Arctic Basin (see Fig. 4). This is the second largest export in the results of the 41-year run, and also agrees quite well with observations by Vinje et al. (1998). This large export is due to a strong anomaly in sea-ice velocity (see Fig. 2). During the 1992–94 period the export is also quite high. The SLP patterns (see Fig. 11a, and d) show an anomalous situation for the 1990–93 period; the large extent of the Icelandic Low in the Arctic stayed that way during a long period (1989–95),

and during the period 1996–97 the Arctic High is still far east of the Arctic Basin (not shown here), allowing a well-developed Transpolar Drift Stream and no sea-ice volume accumulation in the East Siberian Sea.

In the East Siberian Sea, during the 1989–95 period, the sea-ice conditions were lighter than usual, as reported by Maslanik et al. (1996). Maslanik et al. (1996) related these conditions to the large increase in the number of intense winter cyclone events in the late

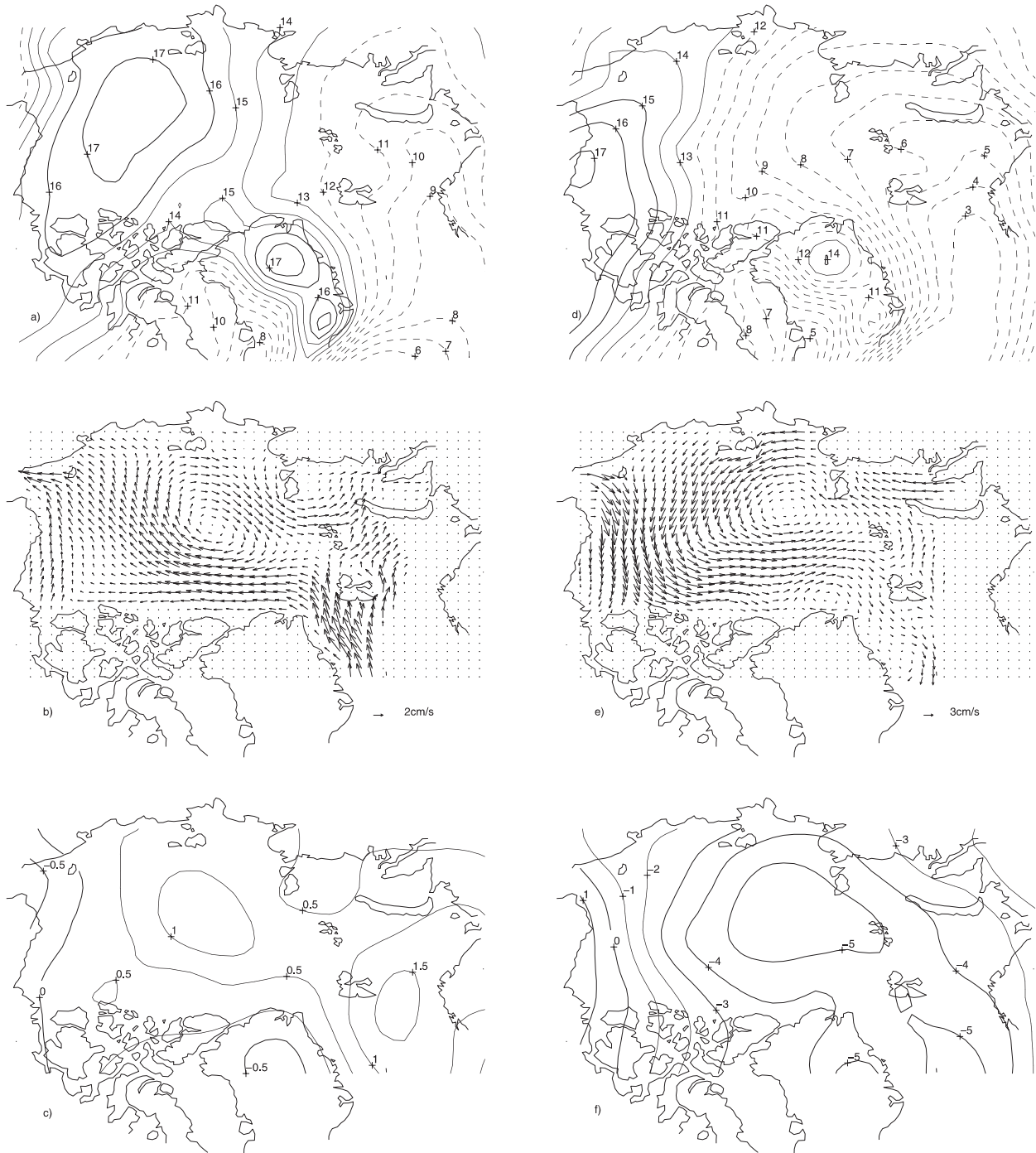


Fig. 10a–f Mean sea-level pressure in hPa (relative to 1000 hPa with SLP contours less than 1013 hPa in dashed lines), anomaly in the mean sea-ice velocity field, and anomaly in the mean sea-level pressure field in hPa for the **a–c** 1985–88 period, and **d–f** the year 1989

1980s in North Atlantic and North Pacific, as reported by Lambert (1996). This last result is confirmed by the large increase in the late 1980s of the winter northerly wind stress in the Fram Strait region computed from the NCEP Reanalysis data set (not shown here). This large increase in the number of intense winter cyclone events in the late 1980s was preceded by a significant positive trend for the number of cyclones (Serreze et al. 1993). Also, during the 1989–95 period, the Arctic Oscillation

(AO) index (Thomson and Wallace 1998) was higher than usual, a situation corresponding to a deeper Polar Vortex, which means a more cyclonic atmospheric circulation over the Arctic Basin (more cyclone events). McPhee et al. (1998) related the observed anomalously thin sea-ice and freshening near the center of the Beaufort Gyre during the SHEBA (Surface Heat Budget of the Arctic Ocean) experiment to the deepening of the Polar Vortex and a more cyclonic circulation in the

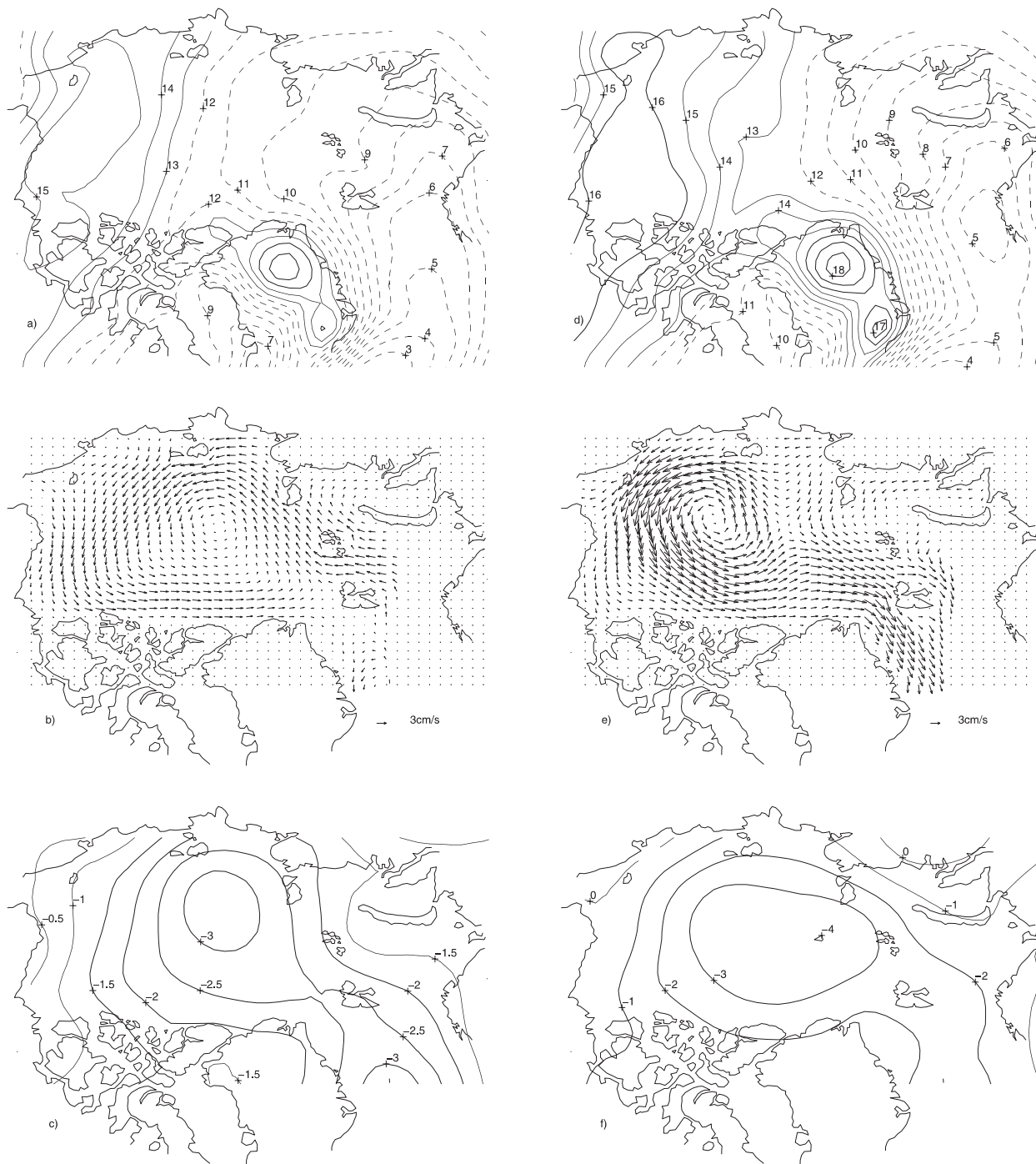


Fig. 11a–f Mean sea-level pressure in hPa (relative to 1000 hPa with SLP contours less than 1013 hPa in *dashed lines*), anomaly in the mean sea-ice velocity field, and anomaly in the mean sea-level pressure field in hPa for **a–c** the 1990–93 period, and **d–f** 1994–95 period

Arctic Basin. These results are in agreement with our results which show a negative anomaly in the SLP pattern for the 1989–98 period, corresponding to a more cyclonic atmospheric circulation over the basin; this drives a more cyclonic sea-ice circulation and also implies no large sea-ice volume formation in the East Siberian Sea.

8 Relation between Fram Strait sea-ice export and the northern North Atlantic Oscillation

An interesting quantity which characterizes the variability of the winter atmospheric circulation in the North Atlantic is the North Atlantic Oscillation (NAO)

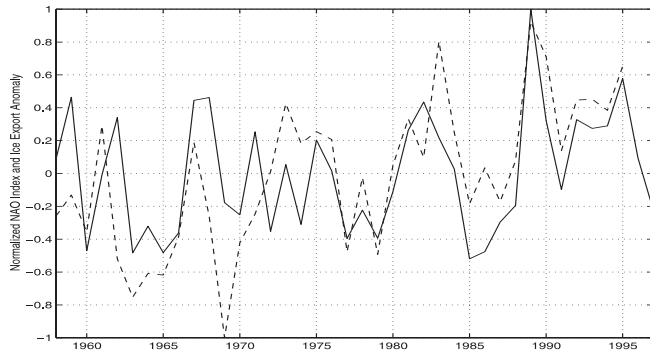


Fig. 12 Normalized NAO index (*dashed line*) versus normalized sea-ice export anomaly through Fram Strait (*solid line*)

index. The sea-ice export through Fram Strait is more in phase with the NAO index after the mid 1970s (see Fig. 12) when there was an increase in the number of intense winter cyclone events in the northern North Atlantic (Lambert 1996). This would correspond on average to a deeper Icelandic Low and would confirm the extended low pressure in the eastern side of the Arctic Basin. It should be noted that the best agreement between the NAO index and the sea-ice export is for the peak in 1989, which is due to an anomaly in sea-ice thickness (see Fig. 2) and not to a large sea-ice velocity, which would be a simple conclusion that would normally be drawn from the Fig. 12. Therefore, it is very important to consider the atmospheric state in the Arctic Basin, which is related to the atmospheric states in the North Pacific and North Atlantic, in order to understand the variability in the Arctic sea-ice cover in the Arctic Basin and the sea-ice export through Fram Strait.

The question of whether a direct link between the NAO and sea-ice export through Fram Strait exists certainly deserves further attention, and this is now under investigation (L.-B. Tremblay 1999, personal communication).

9 Conclusions

The interannual variability of the sea-ice conditions in the Arctic Basin is simulated for the 41-year period 1958–98 using a thermodynamic-dynamic sea-ice model based on granular material rheology. The NCEP Re-analysis data set is used to force the model with climatological monthly-mean surface air temperatures and monthly-mean wind stresses. This approach allows us to focus on the changes in the ice conditions that result from variations in the wind field.

The sea-ice export anomaly through Fram Strait is decomposed into various components; the two main ones are due to the sea-ice velocity and thickness. It is shown that some large sea-ice exports through Fram Strait can be explained by either the thickness anomaly (e.g., in 1989) or the sea-ice velocity anomaly (e.g., in 1995); other exports, on the other hand, can be explained by anomalies in both quantities.

These results underline the importance of the sea-ice evolution in the Arctic Basin, and suggest that the sea-ice export through Fram Strait is not simply dependent on wind in the Fram Strait region. Thus, the interannual variability of the sea-ice volume anomaly in the Arctic Basin is also investigated. The sea-ice export and volume anomalies show related interannual variabilities. In general, large sea-ice exports are preceded by large sea-ice volume anomalies in the Arctic Basin.

The results show that the sea-ice volume anomalies are generally formed in the East Siberian Sea and propagate anticyclonically toward the center of the Arctic Basin, which is consistent with results of Mysak and Venegas (1998). They are then advected directly to the Fram Strait region, generally along, but well offshore from the north Greenland coast, and are subsequently exported through Fram Strait. The hypothesis of the export of multi-year sea-ice from immediately north of the Greenland coast could be supported by the results of the 1985–89 period; however even in this case, the thick ice is mainly formed originally in the East Siberian Sea.

The sea-ice velocity anomalies show that during the sea-ice volume formation periods, the sea-ice is packed more than usual along the East Siberian coast. The SLP patterns show that during these periods the Arctic High is closer to the East Siberian coast. Also, the SLP anomaly patterns imply that the anomalous winds pack the sea-ice in the East Siberian Sea.

During the large export periods, the anomalies in the sea-ice velocity fields show that the sea-ice circulation tends to advect more sea-ice than usual from the center of the Arctic Basin to the Fram Strait region, and hence transports the sea-ice volume anomalies out of the Arctic Basin through Fram Strait. The SLP patterns show that at this time the Arctic High is relocated closer to the Beaufort Sea and the Icelandic Low extends far into the Arctic Basin, which provides for a well-developed Transpolar Drift Stream.

However, during the 1990–98 period, the atmospheric conditions do not allow for the packing of the ice in the East Siberian Sea. The Arctic High is still centered near the Alaska coast and the Icelandic Low is still extends far into the Arctic Basin. In this case, large exports during this period appear to be due to an anomaly in sea-ice velocity. This is consistent with the sea-ice export anomalies results and their decomposition into sea-ice thickness and velocity anomalies, which show that the export is still quite large in the 1990s and that the large export in 1995 (the second largest of the 41-year period) is due not to an anomaly in sea-ice thickness but to an anomaly in sea-ice velocity.

This recent period corresponds to a period of very strong increase in the number of intense winter cyclones in the northern North Atlantic and Pacific (Lambert 1996). In addition, Smith (1998) shows an increase in the length of the melt season of perennial Arctic sea-ice over the same period, and Maslanik et al. (1996) relate these anomalous atmospheric conditions to recent decreases in Arctic summer ice cover.

These results make it even more relevant to consider the sea-ice transport through areas like the Canadian Arctic Archipelago (CAA) straits. With the recent decrease of sea-ice cover and stronger atmospheric circulations, which could be due to global warming, more sea-ice could be transported through the CAA straits into the northern North Atlantic and may thus modify deep water formation in the Labrador Sea.

The sea-ice export anomalies and the NAO index seem to vary together, especially after the late 1980s. At around this time there was an increase in the number of intense winter cyclone events in northern North Atlantic and Pacific. Atmospheric conditions in the Arctic Basin are certainly related to those in the North Atlantic and the North Pacific via the Arctic Oscillation (Thomson and Wallace 1998); thus the Arctic region as a whole should be considered in order to understand the influence of the atmospheric conditions on the sea-ice cover, especially those associated with global warming.

Acknowledgements This work was supported by research grants awarded to L.A.M. from NSERC and AES. G.A. is also indebted to the Centre for Climate and Global Change Research for a Graduate Student Stipend from the FCAR Centre Grant. We are indebted to Halldor Bjornsson and Zhaomin Wang for helpful discussions. L.-B.T. was supported by a NOAA Postdoctoral Fellowship in Climate and Global Change by the UCAR Visiting Science Program.

References

- Aagaard K, Carmack EC (1989) The role of sea ice and other fresh water in the Arctic circulation. *J Geophys Res* 94: 14 485–14 498
- Alekseev GV, Myakoshin OI, Smirnov NP (1997) Variability of the ice transport through the Fram Strait. Available in English. *Meteorol Gidrol* 9: 37–41
- Belkin IM, Levitus S, Antonov J (1998) Great salinity anomalies in the North Atlantic. *Prog Oceanogr* 41: 1–68
- Dickson RR, Meincke J, Malmberg S.-A, Lee AJ (1988) The “great salinity anomaly” in the northern North Atlantic 1968–1982. *Prog Oceanogr* 20: 103–151
- Erlingsson B (1988) Two-dimensional deformation pattern in sea ice. *J Glaciol* 34: 301–308
- Gudkovich ZM (1961) Relation of the ice drift in the Arctic Basin to ice conditions in Soviet Arctic seas (in Russian). *Tr Okeanogr Kom Akad Nauk SSSR* 11: 14–21
- Häkkinen S (1993) An Arctic source for the great salinity anomaly: a simulation of the Arctic ice-ocean system for 1955–1975. *J Geophys Res* 98: 16 397–16 410
- Häkkinen S (1995) Simulated interannual variability of the Greenland Sea deep water formation and its connection to surface forcing. *J Geophys Res* 100: 4761–4770
- Hibler WD III (1979) A dynamic thermodynamic sea-ice model. *J Phy Oceanogr* 9: 815–846
- Hibler WD III, Walsh JE (1982) On modeling seasonal and interannual fluctuations of Arctic sea-ice. *J Phys Oceanogr* 12: 1514–1523
- Houghton LA, Filho LGM, Callander BA, Harris N, Kattentberg A, Maskell K (1996) Climate change 1995. The science of climate change: Contribution of the working group I to the second Assessment Report of the Intergovernmental panel on climate change Cambridge University Press 531 pp.
- Kalnay E, Kanamitsu M, Kistler R, Collins W, Deaven D, Gandin L, Iredell M, Saha S, White G, Woollen J, Zhu Y, Chelliah M, Ebisuzaki W, Higgins W, Janowiak J, Mo KC, Ropelewski C, Wang J, Leemtmann A, Reynolds R, Jenne R, and Joseph D (1996) The NCEP/NCAR 40-Year Reanalysis Project. *Bull Am Meteorol Soc* 77: 437–471
- Kassens H, Dmitrenko I, Rachold V, Thiede J, Timokhov L (1997) Russian and German scientists explore the Arctic’s Laptev Sea and its climate system. *EOS, Transactions, Am Geophys Union* 79: 317–323
- Kwok R, Rothrock DA (1999) Variability of Fram Strait ice flux and North Atlantic Oscillation. *J Geophys Res* 104: 5177–5189
- Lambert SJ (1996) Intense extratropical northern hemisphere winter cyclone events: 1899–1991. *J Geophys Res* 101: 21319–21325
- Levitus S (1994) World ocean atlas 1994, cd-rom data sets, NOAA
- Maslanik JA, Dunn J (1997) On the role of sea-ice transport in modifying Arctic responses to global climate change. *Ann Glaciol* 25: 102–106
- Maslanik JA, Serreze MC, Barry RG (1996) Recent decreases in Arctic summer ice cover and linkages to atmospheric circulation anomalies. *Geophys Res Lett* 23: 1677–1680
- Mauritzen C, Häkkinen S (1997) Influence of sea ice on the thermohaline circulation in the North Atlantic Ocean. *Geophys Res Lett* 24: 3257–3260
- McPhee MGJ, Stanton JH, Morison JH, Martinson DJ (1998) Freshening of the upper ocean in the Arctic: is perennial sea ice disappearing? *Geophys Res Lett* 25: 1729–1732
- Melling H (1999) Exchanges of freshwater through the shallow straits of the North American Arctic. In: Lewis EL (ed) *The fresh water budget of the Arctic Ocean*. Kluwer, Netherlands, (accepted)
- Mysak LA, Manak DK, Marsden RF (1990) Sea ice anomalies observed in the Greenland and Labrador Seas during 1901–1984 and their relation to interdecadal Arctic climate cycle. *Clim Dyn* 5: 111–133
- Mysak LA, Power SB (1992) Sea-ice anomalies in the western Arctic and Greenland-Iceland sea and their relation to an interdecadal climate cycle. *Clim Bull* 26: 147–176
- Mysak LA, Venegas SA (1998) Decadal climate in the Arctic: a new feedback loop for atmosphere-ice-ocean interaction. *Geophys Res Lett* 25: 3607–3610
- Parkinson CL, Comiso JC, Zwally HJ, Cavalieri DJ, Gloersen P, Campbell WJ (1987) *Arctic Sea Ice, 1973–1976. Satellite Passive-Microwave Observations*, 296 pp. NASA, Washington, DC
- Proshutinsky AY, Johnson MA (1997) Two circulation regimes of the wind-driven Arctic Ocean. *J Geophys Res* 102: 12493–12514
- Serreze MC, Box JE, Barry RG, Walsh JE (1993) Characteristics of Arctic synoptic activity, 1952–1989. *Meteorol Atmos Phys* 51: 147–164
- Serreze MC, Maslanik JA, Barry RG, Demaria TL (1992) Winter atmospheric circulation in the Arctic Basin and possible relationships to the great salinity anomaly in the northern North Atlantic. *Geophys Res Lett* 19: 923–926
- Smith DM (1998) Recent increase in the length of the melt season of perennial Arctic sea ice. *Geophys Res Lett* 25: 655–658
- Thomson DWJ, Wallace JM (1998) The Arctic Oscillation signature in the wintertime geopotential height and temperature fields. *Geophys Res Lett* 25: 1297–1300
- Tremblay L-B, Mysak LA, (1997) Modelling sea ice as a granular material, including the dilatancy effect. *J Phys Oceanogr* 27: 2342–2360
- Tremblay L-B, Mysak LA, (1998) On the origin and evolution of sea-ice anomalies in the Beaufort-Chukchi Sea. *Clim Dyn* 14: 451–460
- Vinje TE, Nordlund N, Kvambekk A (1998) Monitoring ice thickness in Fram Strait. *J Geophys Res* 103: 10 437–10 449
- Walsh JE, Chapman WL (1990) Arctic contribution to upper-ocean variability in the North Atlantic. *J Clim* 3: 1462–1473
- Walsh JE, Hibler WD III, Ross B (1985) Numerical simulation of Northern Hemisphere sea-ice variability. *J Geophys Res* 90: 4847–4865